Photoluminescence properties of a Si doped InGaAs/InGaAlAs superlattice

2007 J. Phys.: Condens. Matter 19 086207

(http://iopscience.iop.org/0953-8984/19/8/086207)

IOP PUBLISHING JOURNAL OF PHYSICS: CONDENSED MATTER

J. Phys.: Condens. Matter **19** (2007) 086207 (12pp) doi:10.1088/0953-8984/19/8/086207

Photoluminescence properties of a Si doped InGaAs/InGaAlAs superlattice

E M Lopes[1], J L Duarte[1], I F L Dias[1], L C Poças[1], E Laureto[1] and J C Harmand[2]

[1] Departamento de Física, Universidade Estadual de Londrina, CP 6001, CEP 86051-970, Londrina, Paraná, Brazil
[2] Laboratoire de Photonique et de Nanostructures, Centre National de la Recherche Scientifique (CNRS), Route de Nozay 91460 Marcoussis, France

E-mail: jlduarte@uel.br

Received 6 November 2006, in final form 22 December 2006
Published 9 February 2007
Online at stacks.iop.org/JPhysCM/19/086207

Abstract

In this paper, the optical properties of a Si doped $In_{0.53}Ga_{0.47}As/In_{0.52}Ga_{0.24}Al_{0.24}As$ superlattice (SL) are investigated by using the photoluminescence (PL) technique in the temperature range of 9–300 K. The origins of the optical transitions observed in the spectra are attributed through the analysis of the transition behaviour with temperature and excitation power. The linewidths obtained at 9 and 300 K are smaller than those previously reported in the literature, and the blueshift observed with increasing temperature has a small magnitude, indicating the excellent quality of the sample. The experimental results are compared with theoretical calculations based on the envelope function formalism, with an excellent accordance. The excitonic emission was obtained in the range of 9–300 K, and the applicability of the Varshni, Viña, and Pässler (p-type and ρ-type) models, usually used to describe the variation of the excitonic energy transition as a function of temperature in semiconductor materials, was also analysed.

1. Introduction

Special attention has been paid in the last decades to the research of semiconductor heterostructures regarding the fabrication of optoelectronic devices used in telecommunications systems. In order to maximize the efficiency of the optical fibres used in these systems, it is necessary to use lasers emitting in the low dispersion and low loss regions of these fibres, which are particularly found at wavelengths around 1.3 and 1.55 μm [1].

$In_{1-x-y}Ga_yAl_xAs$ quaternary alloys present some properties that make them suitable for the fabrication of several devices [2–5] used in telecommunications and optoelectronic systems, with some advantages in relation to the alloys initially used: compared with the InGaAsP family, we can mention, for instance, the largest discontinuity of the conduction band [6] and,

in relation to the AlGaAs/GaAs system, it has better electrical properties such as higher electron mobility, larger conduction band discontinuity, lower electron effective mass, and higher electron saturation velocity [7]. These characteristics allowed the design of many devices based on the InGaAlAs system, such as waveguides [8], detectors [9], lasers [10, 11], etc.

In quantum well (QW) structures, the linewidth of the excitonic line is frequently taken as a measure of the sample quality [12]. The tunnelling process, which is characteristic of superlattices, increases the three-dimensional character of these structures, and the sensitivity of the wavefunctions to the interface roughness decreases [13]; as a result, the PL linewidth partially induced by the interface roughness would be slightly reduced [13].

The temperature dependence of the fundamental bandgap energy is an extremely important characteristic of any semiconductor material and it brings forth great interest, mainly from the technological point of view. Some models have been proposed to describe this dependence, but the relation between the physical mechanisms involved with the processes and the parameters used in the expressions of these models has been intensively discussed [14–24]. Among the more used models, we can mention the Varshni [14], Viña [18], and Pässler [19] models.

As for the $In_{1-x-y}Ga_yAl_xAs$ quaternary alloys, few studies of their energy gap and linewidth variation with temperature have been published. Song *et al* [25] have recently discussed the linewidth dependence on temperature in a digital-alloy InGaAs/InGaAlAs multi-quantum well sample, and they observed a relatively narrow (5.7 meV) linewidth at low temperature; however, to our knowledge, there is no systematic analysis of the theoretical models used to describe the energy gap variation with the temperature or the linewidth dependence on temperature for superlattices with InGaAlAs alloy barriers.

In this study, the results obtained by photoluminescence as a function of temperature and excitation power for a sample containing a Si doped InGaAs/InGaAlAs superlattice, grown on InP substrate by molecular-beam epitaxy, are reported. The excitonic transition energy was measured in the whole temperature range of 9–300 K. The origins of the structures that compose the photoluminescence spectra are discussed. It is also verified which is the most appropriate model to adjust the behaviour of the energy 'gap' curves as a function of the temperature for this sample. The observed linewidths are compared with values found in the literature for similar semiconductor structures.

2. Theoretical models

In 1967, Varshni [14] presented an analytical expression to adjust the measured temperature dependence of the energy gap for materials. His empirical expression is

$$E_g(T) = E_g(0) - \alpha_{Var}\frac{T^2}{\beta + T} \tag{1}$$

where $E_g(0)$ is the energy gap at 0 K and α_{Var} and β are the parameters to be determined to adjust the experimental data.

In 1984, Viña *et al* [18] proposed a semi-empirical model to describe the temperature dependence of the energy gap, based on the Bose–Einstein statistical distribution for phonons. The expression proposed by Viña is given by

$$E_g(T) = E_B - a_B\left[1 + \frac{2}{\exp(\Theta_B/T) - 1}\right] \tag{2}$$

where $E_B - a_B$ is the energy gap at 0 K, α_B represents the strength of the electron–phonon interaction and $\Theta_B \equiv \hbar\omega/k_B$ is the characteristic temperature parameter that represents the effective phonon energy on the temperature scale [18].

In 1996, Pässler developed a new analytical four-parameter model (p-type model) to describe the effect of temperature variation on the energy gap in semiconductor materials [19], which is described by the following equation:

$$E_g(T) = E_g(0) - \frac{\alpha\Theta}{2}\left[\sqrt[p]{1+\left(\frac{2T}{\Theta}\right)^p} - 1\right] \tag{3}$$

where $E_g(0)$ is the energy gap at zero Kelvin, $\alpha \equiv S(\infty) \equiv -(\mathrm{d}E/\mathrm{d}T)_{T\to\infty}$ is the high-temperature limit for the forbidden gap entropy (the same parameter as in (1)), Θ is a characteristic temperature parameter of the material representing the effective phonon energy ($\Theta \equiv \hbar\omega/k_B$) in units of absolute temperature [18, 19, 26] (similar to the Θ_B defined for the Viña model), and p is an empirical parameter related to the shape of the electron–phonon spectral functions ($f(\omega)$) [22, 27]. Equation (3) is, actually, an analytical approach of a more general expression which takes into account a spectral function with a power law dependence ($f(\omega) \propto \omega^{\nu}$) on the phonon frequency [27].

By modelling a strongly concave spectral function as a combination of a linear part (related to the contributions of long-wavelength acoustical phonons) plus a singular part (related to the contributions of optical and short-wavelength acoustical phonons), Pässler proposed in 1998 an alternative model for the description of the dependence on temperature of the excitonic transitions (ρ-type model), which is especially useful in the case of narrow quantum wells and short-period superlattices [27]. This analytical representation is

$$E_g(T) = E_g(T=0) - \frac{\alpha\Theta_0}{2}\left[\frac{\rho}{2}\left(\sqrt[4]{1+\frac{\pi^2}{6}\left(\frac{4T}{\Theta_0}\right)^2+\left(\frac{4T}{\Theta_0}\right)^4} - 1\right)\right.$$
$$\left. + (1-\rho)\left(\coth\left(\frac{\Theta_0}{2T}\right) - 1\right)\right]. \tag{4}$$

The $\rho \to 1$ limit corresponds to a linear spectral function and, on the other hand, the $\rho \to 0$ limit corresponds to a singular spectral function and, in this case, equation (4) becomes the Viña expression (equation (2)).

Using the data obtained by Grilli *et al* [28] for the GaAs bulk crystal, Pässler [22] observed that the Varshni and Viña curves are almost indistinguishable for temperatures higher than 100 K. However, for $T < 80$ K there is a clear difference between these curves; in this range, especially for $T < 40$ K, the model proposed by Varshni shows a much faster shrinkage (and stronger curvature) than the experimental curve, overestimating the energy gap for $T = 0$ K. On the other hand, the curve obtained through the expression proposed by Viña shows, in this range, a much slower shrinkage than the curve given by the experimental points, disappearing completely at $T < 20$ K, representing a plateau behaviour and underestimating the energy gap for $T = 0$ K. These results, as well as the better efficiency of the model proposed by Pässler (p-type model, equation (3)), have been frequently observed for many semiconductor materials and structures of semiconductor materials [19, 20, 22, 29–31].

3. Experimental details

The superlattice sample was grown by MBE, in lattice-matched condition, on InP substrate, and it has 52 periods of an 89 Å thick $In_{0.53}Ga_{0.47}As$ well and a 43 Å thick $In_{0.52}Ga_{0.24}Al_{0.24}As$ barrier. The structure was finished with a 43 Å thick InGaAs film. The sample was Si doped, with an impurity concentration of $n \approx 1.2 \times 10^{16}$ cm^{-3}, measured by the Hall effect. The

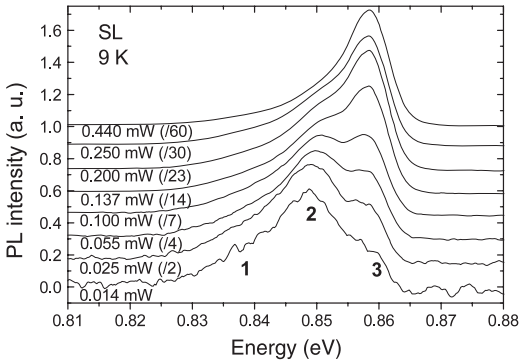

Figure 1. Excitation laser power dependence of the 9 K PL spectra for the SL sample. Only low power PL spectra are shown. The spectra were vertically translated for better visualization.

thicknesses of the wells and the barriers were determined by x-ray measurements, as well as the verification of the lattice-matched condition ($\Delta a/a = 2.2 \times 10^{-4}$).

Photoluminescence measurements were made at temperatures ranging from 2 to 300 K, using a 5145 Å line of an Ar^+ laser as an excitation source. The spectral analysis of the luminescence was carried out by a grating spectrometer (Jarrel Ash 600 1 mm^{-1}) with a 0.50 m focal length and the detection was made by an InGaAs thermo-electrically cooled photodetector using a standard lock-in technique. Temperature-dependent PL measurements were carried out using a cryostat coupled to a He closed circuit. Excitation power dependent PL measurements were obtained at 9 K with laser power ranging between 0.014 and 200 mW, with a 'spot' diameter around 260 μm.

To identify the transitions observed in the PL spectra, the theoretical values of the transitions were calculated using the envelope function formalism [32].

4. Results and discussion

4.1. Recombination process identification

The dependence on the laser excitation power of the PL spectra taken at 9 K and low power values is shown in figure 1. The spectrum obtained with the lowest power shows three emission peaks. Peak 3 (the one with the highest energy) becomes more and more intense as the excitation power is increased, while peaks 1 and 2 become less and less perceptible; for the highest excitation power ($P = 0.440$ mW) only peak 3 and a tail on the low energy side are observed. This behaviour shows that there is saturation, at low excitation intensity, of the channels through which emissions 1 and 2 are occurring, which is a characteristic of the emission by impurities, due to their low density of states.

The PL spectra of the SL sample can be fitted accurately by three Gaussian peaks (figure 2). The dependence on power of the energy peaks, obtained by the fitting procedure for all the spectra presented in figure 1, is shown in figure 3. The data above 0.440 mW, shown in figure 3(c), were obtained directly from the PL spectrum, taking the PL peak energy (without the accomplishment of the fitting procedure).

Figure 3 shows that for excitation power around 0.50 mW peaks 1 and 2 already tend to stabilize at a certain energy value, while peak 3 moves quickly in energy up to excitation powers of approximately 10 mW, showing a stabilization behaviour for larger values.

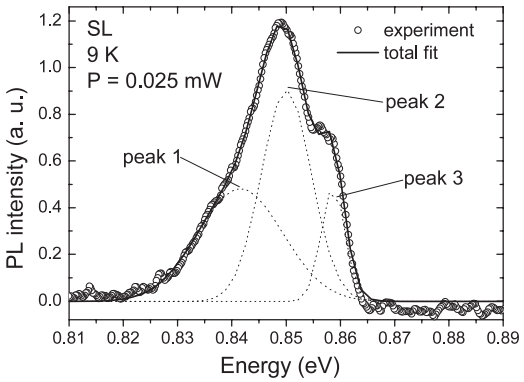

Figure 2. Gaussian fit of the SL PL spectrum. The dotted lines represent the Gaussian peaks used for fitting, while the solid line corresponds to the total fit for the experimental PL data for 0.025 mW excitation.

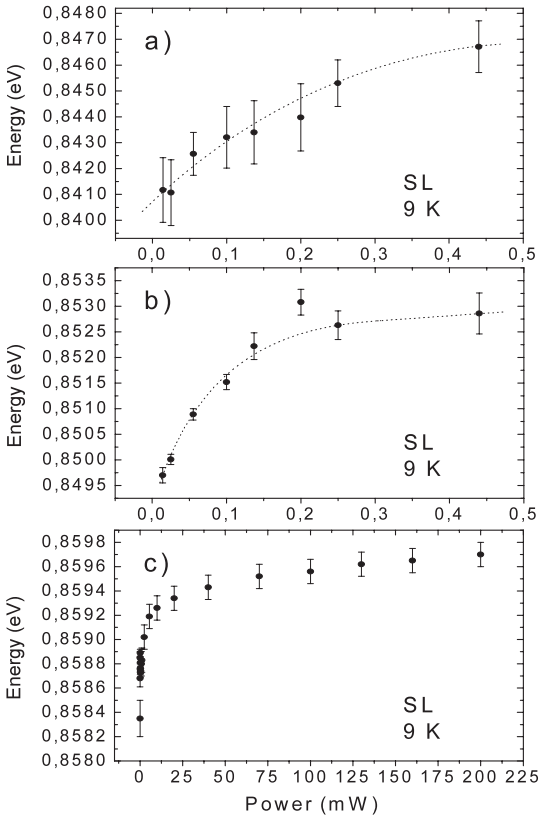

Figure 3. Power dependence of the energy peak obtained by the fitting procedure using three Gaussian peaks: (a) peak 1, (b) peak 2, and (c) peak 3 (the data above 0.440 mW were obtained directly from the PL spectrum considering the energy peak). The error bars were obtained from the computational fit (except for the data above 0.440 mW, for which they were estimated from the energy peak). Note that the power range for peak 3 is larger than for peaks 1 and 2. The dotted lines are used as a guide for the eye.

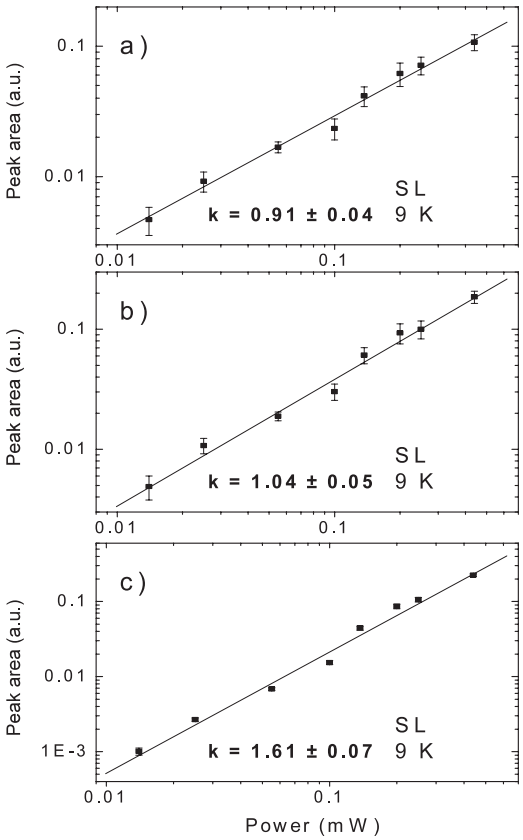

Figure 4. Dependence of the integrated PL intensity on excitation power for the three observed peaks: (a) peak 1, (b) peak 2, and (c) peak 3. The angular coefficient k is less than unity for transitions involving impurities, and between unity and two for excitonic emissions [33].

Peak 3 is attributed to excitonic recombinations and its initial displacement in energy is related to the existence of potential fluctuations. With increasing excitation power, the potential fluctuation states become populated and the generated excitons start occupying higher energy states. When the potential fluctuation states are completely filled, the excitons start occupying free exciton states and, due to the great density of such states, the displacement in energy is small.

Supposing that peaks 1 and 2 originate from transitions involving impurities, they can be of three types: donor–acceptor (D^0–A^0), conduction band–acceptor (e–A^0), or donor–valence band (D^0–hh).

The displacement of peaks 1 and 2 to higher energies as the excitation power increases can be explained by considering the participation of donors and acceptors in these optical recombination processes; i.e., these peaks can be attributed to transitions of the (D^0–A^0) type. In this transition type, as the excitation power increases the more distant (D^0–A^0) pairs saturate because they have very low recombination rates, which favours the emission of closer (D^0–A^0) pairs, resulting in higher energy photons [33].

The analysis of the excitation power (P) dependence of the integrated PL intensity (I), $I\alpha\ P^K$, is also useful for identification of the recombination processes [33]. This analysis, performed from 0.014 to 0.440 mW, is shown in figure 4. The three observed transitions have

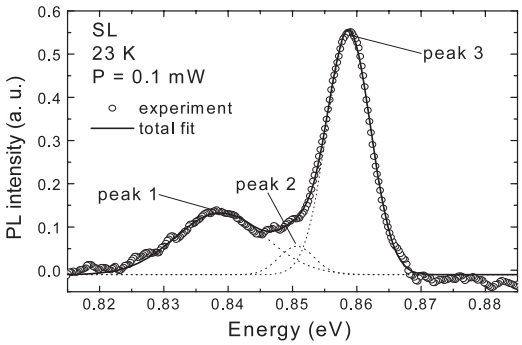

Figure 5. Gaussian fit of the SL PL spectrum at 23 K and 0.1 mW.

presented different behaviours: sublinear behaviour for peak 1 ($k < 1$), approximately linear behaviour for peak 2 ($k \sim 1$), and superlinear behaviour ($k \sim 1.6$) for peak 3. Although the observed behaviour for peak 2 is not clearly sublinear as it should be for an impurity, this was attributed to the uncertainty of the fitting process (in addition to the uncertainty of the integrated PL intensity values), but for peak 3 the behaviour is clearly superlinear, confirming that this peak is related to the excitonic emission.

In order to identify the impurities involved in the transitions, the (e–A^0) luminescence should be collected at low excitation and high temperature conditions, which favours the (e–A^0) transition over the (D^0–A^0) transition. Figure 5 shows the Gaussian fit of the PL spectrum obtained at 23 K and 0.1 mW. For the SL in analysis, the temperature of 23 K should be enough to ionize the present donors. This spectrum presents a clear transition on the lower energy side, which corresponds to peak 1 shown previously in the variation power spectra.

Taking into account the excitonic binding energy, estimated at (4.0 ± 1.0) meV, and the kinetic energy contribution ($1/2k_BT$), one obtains (13.2 ± 2.0) meV and (25.3 ± 2.0) meV for the ionization energies regarding transitions 1 and 2, respectively. These values agree with those obtained by Goetz *et al* [34] for the ionization energies of carbon (13 ± 1 meV) and of silicon (25 ± 1 meV) in the InGaAs 'bulk'. This consideration is quite reasonable, because (i) carbon is one of the most common non-intentional impurities observed in MBE grown samples and (ii) the studied SL is intentionally doped with silicon.

However, Skromme *et al* [35] have attributed the ionization energies of 13.5 and 31.9 meV observed in a GaAs/AlGaAs SL to C acceptors located at barriers and at wells, respectively. One of the reasons for this attribution is the fact that the binding energy calculated for C acceptors in an isolated QW is 32.6 meV at the centre of the well and 14.3 meV for acceptors located at the interfaces [36]. Then, similarly, it is possible that instead of having transition 2 related to the recombination involving C acceptors located at the wells, this transition may be associated with the recombination involving Si acceptors at the barriers, making it impossible to determine unequivocally the origin of the transition related to peak 2. Anyway, peak 1 proves the existence of Si (intentional doping), corroborating the initial assumption for the origin of the transitions: at low temperatures, peaks 1 and 2 are related to (D^0–A^0) transitions because the Si presents an amphoteric character and can be incorporated as donor and/or acceptor.

4.2. Excitonic emission in the temperature range 9–300 K

Figures 6 and 7 show some PL spectra obtained at different temperatures, using 0.1 and 10 mW as excitation power, respectively.

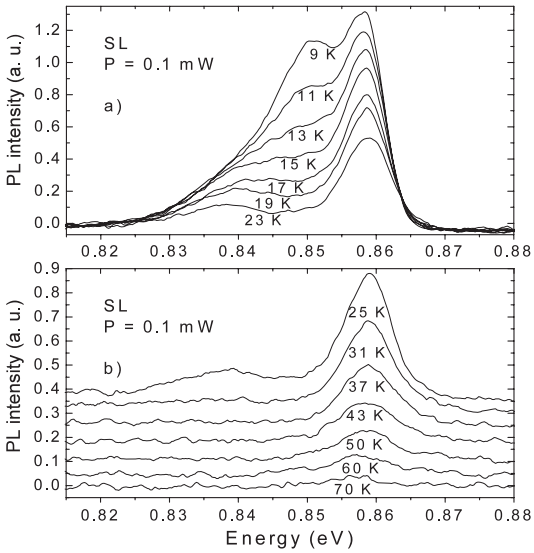

Figure 6. SL PL spectra for the temperature variation at 0.1 mW excitation power.

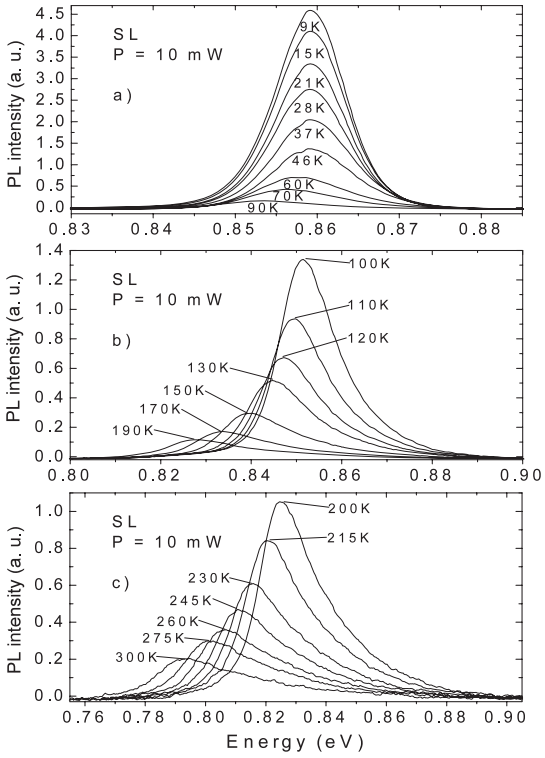

Figure 7. SL PL spectra for the temperature variation at 10 mW excitation power. Note that the energy ranges between the figures are different.

A previous analysis of the spectra shown in figure 6, with $P = 0.1$ mW, leads to the conclusion that peak 2 loses intensity more quickly than peak 1 as the temperature is increased,

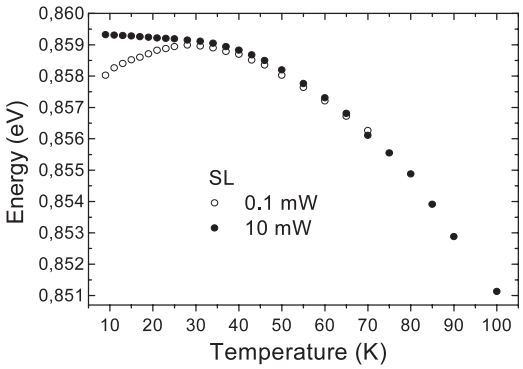

Figure 8. Energy peak variation as a function of temperature for peak 3 at excitation powers of 0.1 and 10 mW.

and that peak 3 persists up to higher temperatures (up to approximately 70 K). This fact reinforces the hypothesis that peaks 1 and 2 are due to impurities and that peak 3 is due to the excitonic emission. In figure 7, for $P = 10$ mW, one can observe an exponential tail on the highest energy side at high temperatures. This asymmetry in the spectrum is related to the statistical thermal distribution of the carriers in the conduction sub-band and it becomes more evident with increasing excitation power due to the participation of a larger number of carriers.

Figure 8 shows the energy peak variation for the excitonic transition (peak 3) as a function of temperature for the excitation powers of 0.1 and 10 mW. The scale is cut at 100 K for better visualization. In the low temperature region, it is possible to observe a small displacement to higher energies ('blueshift') for the curve obtained with 0.1 mW and, above about 28 K, a displacement to smaller energies ('redshift'), in agreement, in the latter case, with the behaviour commonly observed in PL measurements with temperature variation.

As the temperature increases, there is a redistribution of the population of the states relative to the potential fluctuations in such a way that the excitons start occupying higher energies states, resulting in larger recombination energy (emission), which gives rise to the observed 'blueshift.' It is important to point out that during the temperature variation (at low temperatures) there is a competition between the effect of potential fluctuations and the effect of energy 'gap' reduction with the temperature, the later prevailing after about 28 K for the SL sample.

For the curve with $P = 10$ mW, the energy peak variation as a function of temperature shown in figure 8 does not present a 'blueshift'. So, the PL peak obtained with this excitation power and at 9 K gives the appropriate energy value for the SL excitonic transition, 859.3 meV. From the theoretical calculations accomplished through the envelope function formalism [32], the energy value for the e_1–hh_1 transition is 862.1 meV; however, the calculation does not take into account the excitonic binding energy, estimated in (4.0 ± 1.0) meV, which subtracted from the obtained value results in (858.1 ± 1.0) meV. Therefore, an excellent agreement between theory and experimental results is found.

The initial displacement of peak 3 (in energy) with excitation power increasing, observed in figure 3(c), can also be explained in terms of the effect of the potential fluctuations: as the excitation power is increased, the energy states relative to the potential fluctuations, which have a small density of states, become populated and the generated excitons start occupying higher energy states. When the states related to the potential fluctuations are completely filled, the excitons start occupying states of free excitons and, due to the great density of states for these excitons, the energy displacement becomes smaller.

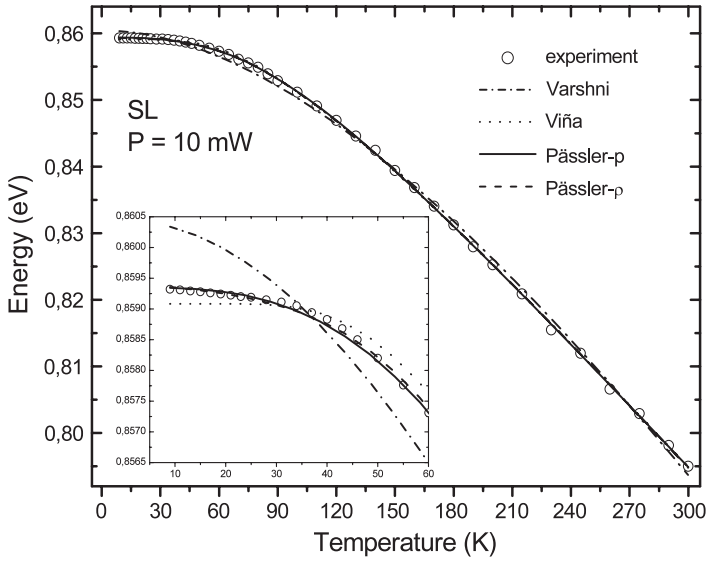

Figure 9. Varshni, Viña, Pässler p-type, and Pässler ρ-type adjustments for the excitonic energy peak variation with the temperature. A maximization of the low temperature region is shown in detail.

The magnitude of the 'blueshift' observed in figure 8 (which is the energy difference between the points at 9 and 28 K) is approximately 1.0 meV, evidencing the good sample quality. One can also come to this conclusion by comparing the obtained linewidths with the values for samples considered as state of the art in the literature. For a digital-alloy InGaAs/InGaAlAs multi-quantum well, Song *et al* [25] obtained the values of 5.7 and 43 meV for the linewidths (FWHM) at 9 and 300 K, respectively. For the studied SL sample these values are ∼5.0 meV (at 0.1 mW, from the Gaussian deconvolution) and 36.1 meV (at 10 mW) for the linewidths at 9 and 300 K, respectively. These results reveal the excellent sample quality because, besides being below the values obtained for the sample considered as state of the art and other values presented in [13], they refer to an intentionally doped SL sample, which contributes to the linewidth broadening of the PL spectra.

4.3. Fit of the experimental curve of the temperature dependence of the excitonic energy peaks through the different theoretical models

Figure 9 shows the accomplished adjustments using the Varshni, Viña, Pässler p-type, and Pässler ρ-type expressions (equations (1), (2), (3), and (4), respectively) for the excitonic energy peak variation with temperature obtained from the PL spectra.

As frequently observed for several semiconductor materials and semiconductor heterostructures [19, 20, 22, 29–31], also for the SL sample studied here, it can be noticed, by analysing the 'inset' for the low temperature region, that the Varshni model overestimates the experimental curve, the Viña model underestimates it, while the Pässler models gives the best adjustments.

In the detail of figure 9 one can also notice that the model proposed by Varshni shows a very strong curvature in the low temperature region, overestimating the experimental data in this range. Then, the Varshni model presents a not so satisfactory adjustment for the SL analysed, as already observed in other studies considering different semiconductor materials

Table 1. Parameter values obtained for the temperature dependence of the PL peak using the Varshni, Viña, Pässler p-type, and Pässler ρ-type models.

Model	$E_g(0)$ (meV) $E_B - a_B$ (meV)	α (10^{-4} eV K^{-1}) a_B (meV)	β (K) Θ (K)	p	ρ	S^2 (meV)^2
Varshni	860.4 ± 0.2	5.5 ± 0.4	445 ± 52	—	—	0.644
Viña	859.1 ± 1.2	39.43 ± 0.63	240 ± 3	—	—	0.076
Pässler p	859.4 ± 0.1	3.20 ± 0.03	199 ± 4	3.1 ± 0.1	—	0.046
Pässler ρ	859.4 ± 0.1	3.30 ± 0.03	272 ± 9	—	0.17 ± 0.04	0.054

and structures [21, 27, 29]. The Viña model, in spite of considering the Bose–Einstein statistical distribution in its formulation, gives a much lower curvature in the low temperature range, which entirely disappears for $T < 30$ K, underestimating the experimental data. This plateau behaviour, characteristic of the Viña model, evidences the absence of any dependence of the 'power type' (T^p) for the dependence on temperature of the excitonic energy transition. This can be explained by the fact that this model does not include the contribution of the long wavelength acoustical phonons (important at low temperatures) to the temperature dependence of the excitonic energy transition. The Pässler models present the best adjustments because, besides being a four parameter model (unlike the Varshni and Viña models, with three parameters), they are also based on phonon spectral functions which take into account the effective contribution from the optical and acoustical phonon branches.

Table 1 presents the parameter values obtained from the adjustments using the four models. In this table, besides the parameters involved in the theoretical models, the value of the variance S^2 is also shown, which is used as an evaluation criterion for the quality of the reproduction of the curve described by the experimental data [29]. The expression obtained by using the Pässler p-type model minimizes S^2, despite the fact that the Pässler ρ-type model also presents a small variance relative to the other two models.

The ρ value, 0.17, obtained from the Pässler ρ-type model indicates that the contribution of the acoustic phonons is very small, i.e., the reduction of the excitonic transition energy with increasing temperature, observed for the studied SL, is mainly due to optical phonon contributions.

5. Summary

The results obtained through the PL measurements with power variation at low temperatures allowed the classification of transitions 1 and 2 (of lower energies) as being caused by impurities, and transition 3 as an excitonic recombination. Such measurements, together with the temperature variation at different excitation powers, showed that the potential fluctuations are of small magnitude, which, together with the observation of relatively narrow linewidths, indicates the excellent sample quality.

The temperature variation allowed the formulation of two possibilities for identification of low energy transitions (1 and 2): (i) transition 1 (lower energy) is related to the Si acceptors and transition 2 to the C acceptors and (ii) transition 1 is related to the Si acceptors located at the wells and transition 2 to the Si acceptors located at the barriers.

Adjusting the data obtained for the temperature variation at 10 mW by the Varshni, Viña, Pässler p-type, and Pässler ρ-type expressions, it was verified that, as well as in other works with different structures, the Varshni model overestimates the experimental curve, the Viña model underestimates it, and the Pässler models result in the best adjustments for this SL. The use of the Pässler ρ-type model has shown that the effective contribution for the excitonic

energy transition reduction with the temperature is mainly due to the optical phonons for the studied SL.

Acknowledgments

The authors would like to acknowledge the financial support granted by the Brazilian agencies Coordenação de Aperfeiçoamento de Pessoal de Nível Superior (CAPES), Conselho Nacional de Desenvolvimento Científico e Tecnológico (CNPq), Fundação Araucária de Apoio ao Desenvolvimento Científico e Tecnológico do Paraná (Fundação Araucária), and Fundação Banco do Brasil (FBB).

References

[1] Nagayama K, KaKui M, Matsui M, Saitoh T and Chigusa Y 2002 *Electron Lett.* **38** 1168
[2] Zhu X, Pavlidis D, Zhao G, Bove P, Lahrèche H and Langer R 2003 *IEICE Trans. Electron.* **E86-C** 2010
[3] Champagne A, Lestrade M and Maciejko R 2004 *Photonics North 2004: Optical Components and Devices*; *Proc. SPIE* **5577** 144
[4] Dahdah N E, Decobert J, Shen A, Bouchoule S, Kazmierski C, Aubin G, Benkelfat B E and Ramdane A 2004 *IEEE Photon. Technol. Lett.* **16** 2302
[5] Paoletti R *et al* 2006 *J. Lightwave Technol.* **24** 143
[6] Mereuta A, Mircea A, Rudra A, Iakovlev V, Syrbu A, Suruceanu G, Berseth C A, Caliman A, Leifer K and Kapon E 2003 *10th European Workshop on MOVPE (Lecce, Italy, PS.V.)* p 13
[7] Fan J C and Chen Y F 1996 *J. Appl. Phys.* **80** 1239
[8] Shimizu H and Nakano Y 2006 *J. Lightwave Technol.* **24** 38
[9] Jelen C, Slivken S, Guzman V, Razeghi M and Brown G J 1998 *IEEE Quantum Electron.* **34** 1873
[10] Xia J, Hoan O B, Lee S G and Lee E H 2005 *Opt. Laser Technol.* **37** 125
[11] Sirenko A A, Kazimirov A, Huang R, Bilderback D H, O'Malley S, Gupta V, Bacher K, Ketelsen L J P and Ougazzaden A 2005 *J. Appl. Phys.* **97** 063512
[12] Jung P S, Jacob J M, Song J J, Shang Y C and Tu C W 1989 *Phys. Rev.* B **40** 6454
[13] Hillmer H, Lösch R and Schalapp W 1997 *J. Cryst. Growth* **175/176** 1120
[14] Varshni Y P 1967 *Physica (Utrecht)* **34** 194
[15] Thurmond C D 1975 *J. Electrochem. Soc.* **122** 1133
[16] Allen P B and Cardona M 1981 *Phys. Rev.* B **23** 1495
[17] Manoogian A and Wolley J C 1984 *Can. J. Phys.* **62** 285
[18] Viña L, Logthetidis S and Cardona M 1984 *Phys. Rev.* B **30** 1979
[19] Pässler R 1996 *Phys. Status Solidi* b **193** 135
[20] Pässler R 1996 *Solid-State Electron.* **39** 1311
[21] Pässler R and Oelgart G 1997 *J. Appl. Phys.* **82** 2611
[22] Pässler R 1997 *Phys. Status Solidi* b **200** 155
[23] Pässler R 2000 *J. Appl. Phys.* **88** 2570
[24] Pässler R 2002 *Phys. Rev.* B **66** 085201
[25] Song J D, Choi W J, Kim J M, Chang K S and Lee Y T 2004 *J. Cryst. Growth* **270** 295
[26] Gopalan S, Lautenshlager P and Cardona M 1987 *Phys. Rev.* B **35** 5577
[27] Pässler R 1998 *J. Appl. Phys.* **83** 3356
[28] Grilli E, Guzzi M, Zamboni R and Pavesi L 1992 *Phys. Rev.* B **45** 1638
[29] Lourenço S A, Dias I F L, Laureto E, Duarte J L, Toginho Filho D O, Meneses E A and Leite J R 2001 *Eur. Phys. J.* B **21** 11
[30] Lourenço S A, Dias I F L, Duarte J L, Laureto E and Iwamoto H 2001 *Superlatt. Microstruct.* **29** 225
[31] Lourenço S A, Dias I F L, Duarte J L, Laureto E, Poças L C, Toginho Filho D O and Leite J R 2004 *Braz. J. Phys.* **34** 517
[32] Bastard G 1981 *Phys. Rev.* B **24** 5693
[33] Pavesi L and Guzzi M 1994 *J. Appl. Phys.* **75** 4779
[34] Goetz K H, Bimberg D, Jürgensen H, Selders J, Solomonov A V, Glinskii G F and Razeghi M 1983 *J. Appl. Phys.* **54** 4543
[35] Skromme B J, Bhat R and Koza M A 1988 *Solid State Commun.* **66** 543
[36] Masselink W T, Chang Y C and Morkoc H 1985 *Phys. Rev.* B **32** 5190